

A99-36846

AIAA 99-4329

MOTION FIDELITY CRITERIA FOR ROLL-LATERAL TRANSLATIONAL TASKS

Julie Mikula*

NASA Ames Research Center
Moffett Field, California

William W.Y. Chung*

Logicon Information Systems & Services
Moffett Field, California

Duc Tran†

NASA Ames Research Center
Moffett Field, California

Abstract

A systematic effort investigating the motion cueing dependencies for coordinated roll-lateral tasks was designed for this study. Previous studies suggested a possible criterion to determine required motion fidelity. This experiment was expanded to confirm the previously suggested criteria by investigating a full range of rotational and translational motion attenuation and phase distortion. Two translational tasks were developed: (1) a helicopter making a 20-ft translation in hover, and (2) a fixed-wing jet making a 20-ft translation at a cruising speed of 250 knots. Both aircraft had desired handling qualities. Motion fidelity ratings and handling qualities ratings were collected as the subjective data. The results were consistent with and extended the previously suggested fidelity criteria for coordinated roll-lateral tasks.

Nomenclature

F_{BO}	lateral stick breakout force, lb
F_{lat}	lateral stick force gradient, lb/in
g	gravitational acceleration, ft/sec ²
K_{lat}	lateral motion washout filter gain, n.d.
K_p	roll motion washout filter gain, n.d.
$L_{\delta_{lat}}$	helicopter roll control power, rad/sec ² /in
L_p	helicopter roll acceleration due to roll rate, 1/sec
p	helicopter roll angular rate, rad/sec
\dot{p}	helicopter roll angular acceleration, rad/sec ²
r_z	vertical displacement between pilot abdomen and the simulator rotational center, positive downward, ft
v	helicopter translational velocity, y-body axis, ft/sec

\dot{v}	helicopter translational acceleration, y-body axis, ft/sec ²
δ_{lat}	pilot lateral stick input, in
ϕ	aircraft roll attitude, rad
$\dot{\phi}$	aircraft roll attitude rate, rad/sec
ω_p	roll motion washout filter frequency, rad/sec
ω_y	lateral motion washout filter frequency, rad/sec
ζ_p	roll motion washout filter damping ratio, n.d.
ζ_y	lateral motion washout filter damping ratio, n.d.

Introduction

The required motion fidelity has been a critical issue for the simulation community as applications for ground-based flight simulations have expanded. It is known that the fidelity of the ground-based flight simulation is dependent on the simulated aircraft characteristics, tasks, and hardware dynamic performance. The interactions among these elements is the primary reason that motion tuning for the motion-based flight simulators still heavily relies on subjective adjustment.¹

Efforts have been developed to establish motion cueing fidelity criteria. Sinacori² proposed a Motion Fidelity Scale (MFS), which correlated pilot opinion with the motion platform magnitude attenuation and phase distortion. His results were based on a slalom maneuver with a top speed of 60 knots, banking turns up to ± 60 degrees and normal load factors to 2 g's, and a precision hover. Jex³ presented a subjective correlation to the motion magnitude attenuation and phase distortion based on a 15 degrees bank-and-stop fighter maneuver with a fully coordinated aircraft. He developed a criterion on the sway motion necessary to keep the spurious side force cues (from the rolling motion) small enough to prevent pilot objections. Schroeder⁴ subsequently investigated the motion gain dependency of the sway motion relative to the roll motion with no washout filter applied. Chung⁵ then combined the previous criteria which tied the roll and lateral motion washout filter characteristics together as shown in Figure 1.

* Member AIAA.

† Senior Member of AIAA

This study was developed to further confirm the Figure 1 criterion by examining the motion filter conditions more thoroughly, with additional pilots and tasks.

Experiment Description

Aircraft Models

Two aircraft, a helicopter and a fixed-wing jet, were developed from a generic, two degree-of-freedom model. This input was effectively roll rate command and the lateral response was fully coordinated as given by equation 1,

$$\begin{bmatrix} \dot{p} \\ \dot{v} \\ \dot{\phi} \end{bmatrix} = \begin{bmatrix} L_p & 0 & 0 \\ 0 & 0 & g \\ 1 & 0 & 0 \end{bmatrix} \begin{bmatrix} p \\ v \\ \phi \end{bmatrix} + \begin{bmatrix} L_{\delta_{lat}} \\ 0 \\ 0 \end{bmatrix} \delta_{lat} \quad (1)$$

The model values and cockpit stick characteristics are shown in Table 1. The control power was chosen so that both aircraft would have the same steady state roll rate per stick force input. The rotational center for both model was chosen at the pilot's abdomen.

The objective to use two different force characteristics is to determine if there are any differences in motion fidelity requirements between rotary wing tasks with a lighter stick force gradient at 1 lb/in and fixed wing tasks with a heavier stick force gradient at 2 lb/in.

Task- Helicopter

The helicopter tasks was a 20-ft lateral translation performed at a constant altitude of 25 ft as shown in Figure 2. Pilots had clear dimensional information from evenly spaced windows and ground texture. The task started in a hover and then translated 20-ft to the right, followed by 20 seconds of hover station keeping in a medium level of sum-of-sines disturbance, Table 2. This disturbance was summed directly with the pilot's control input. The desired time to complete the lateral translation was 7 seconds. The adequate completion time was 11 seconds. The desired station keeping position error was ± 2 ft, which matched the visual scene window width for easy identification. The adequate position error was ± 5 ft.

Task- Fixed-wing Jet

The fixed-wing jet used the scene shown in Figure 3. At a cruising speed of 250 Knots and an altitude of 1000 ft, the pilot was instructed to translate from the left drop tank of the leading aircraft to the drop tank at the right. In contrast with the helicopter task, pilots had a good horizon cueing reference but with less dimensional information. The same transition time performance criteria as well as the position error criteria was used as with the helicopter task. The aircraft was positioned at the same distance from the leading aircraft as the helicopter was positioned in front of the building. Note that the model did not allow a heading change, which would be small in this maneuver. The

primary differences between this task and the helicopter task was the fighter-like stick force gradient and the substantially different visual cues.

Test Facilities

The roll and lateral motion axes of the Vertical Motion Simulator (VMS), Figure 4, provided ± 18 degrees of bank and 40 ft of lateral travel. The motion and visual responses were measured using the frequency response identification technique called CIPHER^{®7} along with an Image Dynamic Measurement System (IDMS)⁸. Figure 5 illustrates the visual measurement setup. A Gaussian white noise input was fed into the control input and the visual and motion responses were recorded for analysis. The helicopter model's roll rate response, visual response, and platform motion responses are shown in Figure 6. The visual response approximates a 60 msec pure time delay over that of the math model. The VMS's roll motion response and lateral motion response are shown in Figure 7, which shows a well matched motion system response, as recommended⁹.

Test Configuration and Procedures

The motion drive algorithm was comprised of two conventional second order high-pass washout filters, as shown in Figure 8. Both had damping ratios, ζ_p and ζ_y of 0.7. A roll washout filter generated the roll motion commands, and a lateral washout filter provided the lateral motion to mitigate the leans due to the roll motion. Four roll washout filter characteristics, Figure 9, with varying roll filter frequencies, ω_y were selected to represent low, medium, and high motion fidelity as predicted and defined in Reference 5. Six lateral washout filters with variations in magnitude, K_{lat} , and phase distortion, ω_y , as shown in Figure 9, were also developed to span medium and high fidelity according to Reference 5. The low-fidelity translational motion region was not tested due to the fact that both References 3 and 4 have adequately validated that region to be unacceptable.

The gain and washout filter frequencies used for all roll and lateral configurations are shown in Tables 3 and 4. All combinations of Table 3 and Table 4 were tested. Test configurations were randomly ordered and pilots flew each configuration at least three times before giving their ratings. Annunciators inside the cockpit were used to inform pilots of their tasks performance for both the translational time and station-keeping position error. Five experienced pilots, which included two Navy Test Pilot School instructors, two NASA test pilots, and one retired NASA test pilot, participated in this investigation. Pilots were asked to give handling qualities ratings (HQRs)⁶ and motion fidelity scale (MFS) ratings as shown in Table 5.

Results

Test data were analyzed according to the roll motion configurations as shown in Table 3, and in Figure 9. The first group, A1, was analyzed for full roll motion (A1), i.e., the simulator bank angle followed the helicopter bank angle without any magnitude attenuation and phase distortion. For this condition, the variables were: lateral gain (K_p) and lateral phase distortion by changing the washout filter frequency (ω_p).

The second group, was analyzed for the attenuated roll motion with magnitude gain of 0.6 and three levels of phase distortion, i.e., phase distortion at 1 rad/sec of 20 degrees, 43 degrees, and 80 degrees, or test points A2, A3, and A4 from Figure 9 respectively. For this roll motion gain, the variables were roll motion phase distortion, (by changing ω_p), lateral motion phase distortion (by changing ω_y), and lateral motion gain (K_{lat}).

The observed levels of significance (p-values) were determined for these two groups of data, as shown in Table 6. A p-value is the probability of being incorrect in stating that an experimental factor (such as translational phase distortion) is causing the variation of the data (such as the handling qualities rating) rather than the variation being due to random effects. Typically, when the p-value is less than 0.05 (5 chances in 100 of making an error), the results are deemed statistically significant.

Helicopter - Full roll motion (A1):

The results from Table 6 show there is a significant effect due to the lateral motion gain on the average MFS ($p=0.037$) and HQR ($p=0.042$). The average MFS degraded from 1.7 to 1.3, and HQR degraded from 5.2 to 5.6 as the lateral motion gain (K_{lat}) was reduced from 0.8 to 0.5.

The data also show there is a significant effect due to the combination of the lateral motion gain and lateral washout filter frequency (lateral phase distortion) on the average MFS ($p=0.004$) and HQR ($p=0.023$). Figure 10 shows the average motion fidelity scale rating degraded as the lateral washout filter frequency (ω_y), increased from 0.25 to 0.9 with the interaction from the lateral motion gain.

The results suggest when the roll motion cues match the visual cues, there is a benefit to minimize the lateral phase distortion and use as much lateral motion gain to mitigate the leans due to the roll motion. However, when lateral phase distortion is high ($\omega_p \geq 0.5$), little benefit is gained with using larger lateral motion gain. This is consistent with the Reference 5 findings.

Helicopter - Attenuated roll motion (A2, A3, A4):

There were significant motion fidelity dependencies found due to the roll motion phase distortion ($p=0.026$), and the lateral motion phase distortion ($p=0.022$). Figure 11 shows the averaged MFS degraded as

the roll motion phase distortion (ω_p) increased. Figure 12 shows the averaged motion fidelity scales degraded as the lateral washout filter frequency (ω_y) increased from 0.25 to 0.9.

From Table 6, the handling qualities was found to be affected by the lateral motion phase distortion ($p=0.022$) only. Figure 12 shows the average HQR degraded as the lateral washout filter frequency increased from 0.25 to 0.9.

There is also a marginal motion fidelity dependency ($0.1 > p > 0.05$) found due to the lateral motion gain ($p=0.072$) and the combination of the roll phase distortion and the lateral gain ($p=0.091$). As shown in Figure 13, the average motion fidelity scales improved when the roll motion phase distortion is relatively small ($\omega_p=0.25$ and 0.5) when $K_{lat}=0.8$. However, for the largest roll phase distortion ($\omega_p=0.9$), the larger lateral motion gain had a negative effect on the motion fidelity. The rationale may lie in the distorted roll motion cues were simply reinforced by the erroneous side force cues.

The results suggest that motion fidelity is dependent on the roll motion phase distortion, the lateral motion phase distortion, and the lateral motion gain. The results suggest there is a benefit to keep both the roll motion phase distortion and the lateral motion phase distortion as low as possible, and provide as much lateral motion gain as possible when low phase distortions are applied. This is consistent with Reference 5 findings.

By defining high motion fidelity as the mean-MFS ≥ 2.5 , medium motion fidelity as the mean-MFS between 2.5 and 1.5, and the low motion fidelity as the mean-MFS less than 1.5, the average MFS from the helicopter task are compared with the criteria proposed in Reference 5 as shown in Figure 14. The results show good match in the expected high and medium motion fidelity regions. In the expected low motion fidelity region, only 4 out of 10 test outcomes match the predicted fidelity. For those unmatched low motion fidelity cases, the trend of degradation and the average MFS are still leaning toward the low motion fidelity.

Fixed-Wing

Due to limited time available, only three roll motion configurations and four lateral motion configurations were evaluated. The three roll motion configurations were A1, A2, and A3; and the four lateral motion configurations were T1, T4, T5, and T6 as shown in Figure 9.

Fixed Wing - Full roll motion (A1):

The average motion fidelity degraded as the lateral motion gain decreased from 0.8 to 0.5 as shown in Figure 15. The average motion fidelity degraded as the lateral phase distortion increased as shown in Figure 16. These results are consistent with the helicopter task. The average

HQR shows the same consistency as shown in the average HQR graphs in Figure 15 and 16.

Fixed-Wing - Attenuated roll motion (A2, A3):

Both the averaged MFS and HQR degraded as the roll motion phase distortion increased as shown in Figure 17. Both the averaged MFS and HQR also degraded as the lateral motion phase distortion increases. Figure 18 shows the MFS and HQR degrading as the lateral washout frequency (ω_y) increased which is also consistent with the helicopter task results..

In general, results from this evaluation are quite consistent with the helicopter hover task. This is significant in establishing that even with different control power settings (0.67 vs. 1.33 rad/sec²/in.), different stick force gradients (1.0 vs. 2.0 lb/in.) and different tasks and visuals scenes the results were consistent.

Conclusions

1) When using roll and lateral motion filters in a coordinated task, the roll phase distortion, lateral phase distortion, and lateral gain were shown to have effects to the motion fidelity. The findings suggest there is a benefit to keep the phase distortion, i.e., the washout filter frequency, of both washout filters small to improve the motion fidelity. In addition, the findings show there is a benefit to keep the lateral gain large when the phase distortion is small to improve the motion fidelity

2). The findings support the fidelity criteria proposed in Reference 5.

References

¹Grant, P.R. and Reid, L.D.: "Motion Washout Filter Tuning: Rules and Requirements," AIAA Flight Simulation Technologies Conference, August 1995.

²Sinacori, J. B.: "The Determination of Some Requirements for a Helicopter Flight Research Simulation Facility," NASA CR 152066, September 1977.

³Jex, H.R., Jewell, W.F., Magdaleno, R.E., and Junker, A.M., "Effects of Various Lateral-Beam Washouts on Pilot Tracking and Opinion in the Lamar Simulator," AFFDL-TR-79-3134, pp. 244-266.

⁴Schroeder, J.A. and Chung, W.Y.: "Effects of Roll and Lateral Flight Simulation Motion Gains on a Sidestep Task," American Helicopter Society's 53rd Annual Forum, April 1997.

⁵Chung, W.Y., Robinson, D.J., Wong, J., and Tran, D.: "Investigation of Roll-Lateral Coordinated Motion Requirements with a Conventional Hexapod Motion Platform," AIAA Motion and Simulation Technologies Conference, AIAA-98-4172, August 1998.

⁶Cooper, G. E.; and Harper, R. P., Jr.: "The Use of Pilot Rating in the Evaluation of Aircraft Handling Qualities," NASA TN D-5153, April 1969.

⁷Tischler, M. B., Cauffman, M.G.: "Frequency-Response Method for Rotorcraft System Identification: Flight Applications to BO-105 Coupled Rotor/Fuselage Dynamics," Journal of the American Helicopter Society, Vol 37, No 3, pgs 3-17, July 1992.

⁸Lehmer, R.D., and Chung, W.Y.: "Image Dynamic Measurement System (IDMS-2) for Flight Simulation Fidelity Verification," AIAA Modeling and Simulation Conference, AIAA 99-4035, August 1999.

⁹Chung, W.Y. and Schroeder, J.A.: "Visual and Roll-Lateral Motion Cueing Synchronization Requirements for Motion-Based Flight Simulations," American Helicopter Society's 53rd Annual Forum, April 1997.

Table 1. Simulated aircraft response and force characteristics

Aircraft	L_p	$L_{\delta_{lat}}$	F_{lat}	F_{BO}
Helicopter	- 4	0.67	1.0	0.5
Fixed Wing	- 4	1.33	2.0	0.5

Table 2. External disturbance

Frequency (rad/sec)	0.28	0.49	0.8	1.5	2.67	4.6	8.5
Amplitude (in)	0.002	0.006	0.014	0.032	0.054	0.068	0.06

Angular configuration	Motion Gain, K_p	Washout filter Frequency, ω_p (rad/sec)	Gain	@ 1 rad/sec Phase distortion (deg)
A1	1.0	0.0001	1	0.0
A2	0.6	0.25	0.6	20
A3	0.6	0.5	0.58	43
A4	0.6	0.9	0.47	80

Table 4. Coordinated lateral motion washout filter configurations

Coordinated translation configuration	Motion Gain, K_{Lat}	Washout filter Frequency, ω_y (rad/sec)	Gain	@ 1 rad/sec Phase distortion relative to angular motion (deg)
T1	0.8	0.25	0.8	20
T2	0.8	0.5	0.78	43
T3	0.8	0.9	0.63	80
T4	0.5	0.25	0.5	20
T5	0.5	0.5	0.49	43
T6	0.5	0.9	0.4	80

Table 5. Motion fidelity scale

	Description	Score
High Fidelity	Motion sensations are not noticeably different from those of visual flight	3
Medium Fidelity	Motion sensations are noticeably different from those of visual flight, but not objectionable	2
Low Fidelity	Motion sensations are noticeably different from those of visual flight and objectionable	1

Table 6. Observed levels of significance (p)

Full Roll Motion	Motion Fidelity Scale	Handling Qualities Rating
Lateral gain	0.037	0.042
Lateral phase distortion	0.067*	no significance
Lateral gain & lateral phase distortion	0.004	0.023
Attenuated Roll Motion		
Roll phase distortion	0.026	no significance
Lateral phase distortion	0.022	0.022
Lateral gain	0.072*	no significance
Roll phase distortion & lateral gain	0.091*	no significance

*Marginally significant

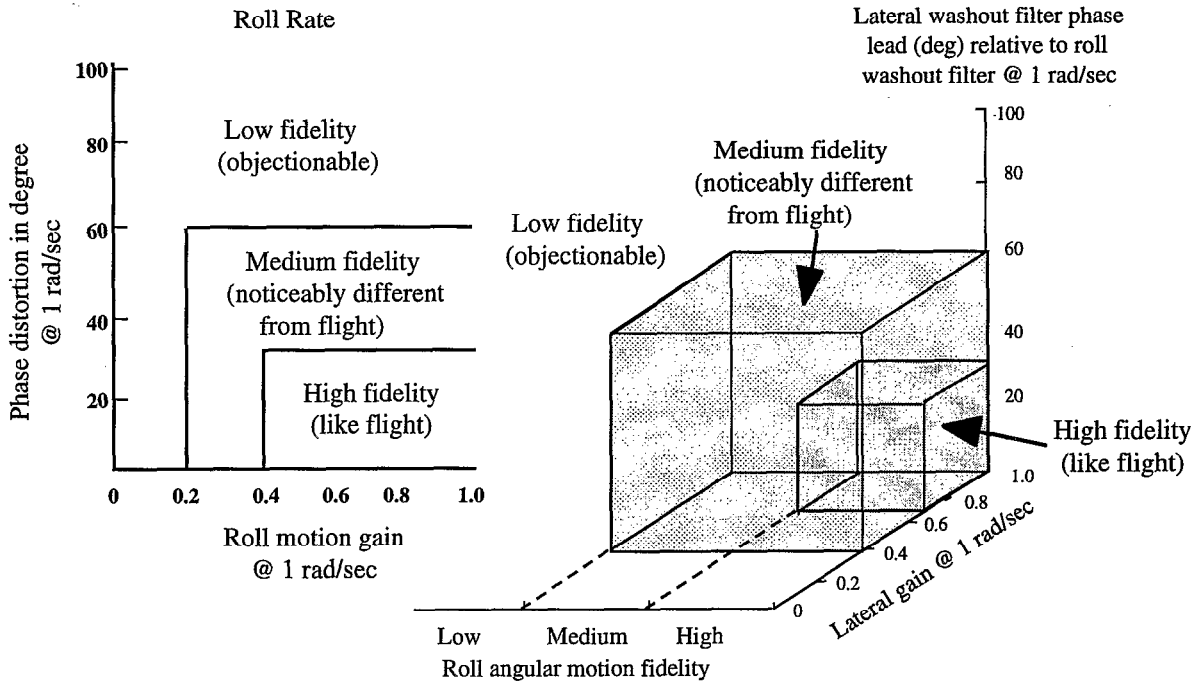


Figure 1. Motion fidelity criteria for the roll-lateral task

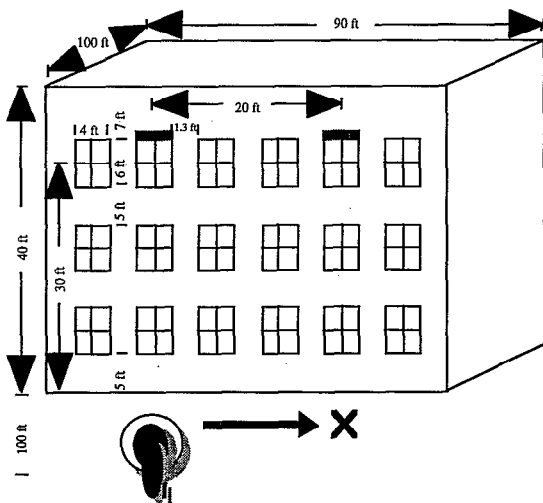


Figure 2. Lateral translational task for the helicopter

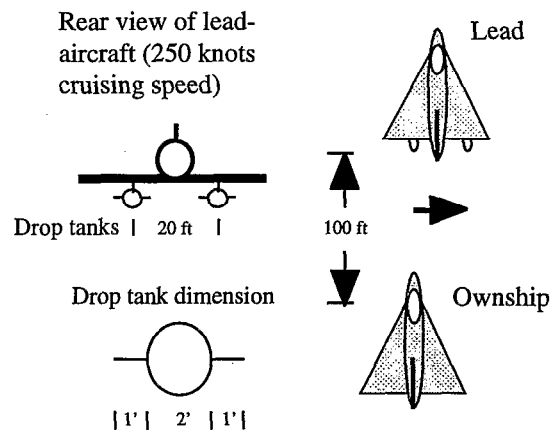


Figure 3. Formation flight task for the fixed-wing jet

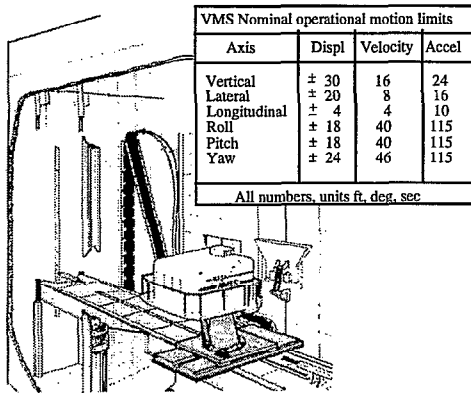


Figure 4. Vertical Motion Simulator (VMS)

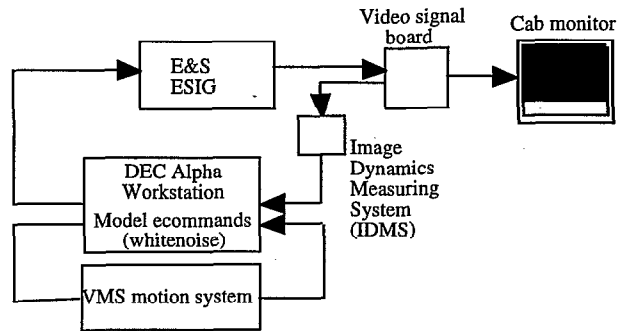


Figure 5. Visual delay measurement setup by white noise or frequency sweep

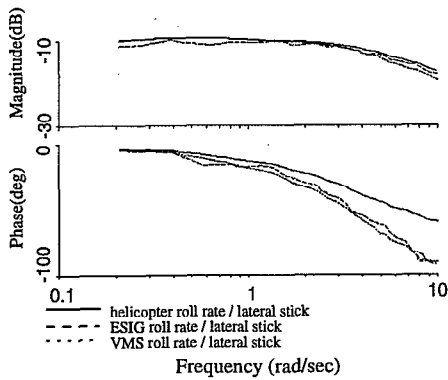


Figure 6. Frequency response of the test model roll rate response, visual throughput response, and the roll motion response

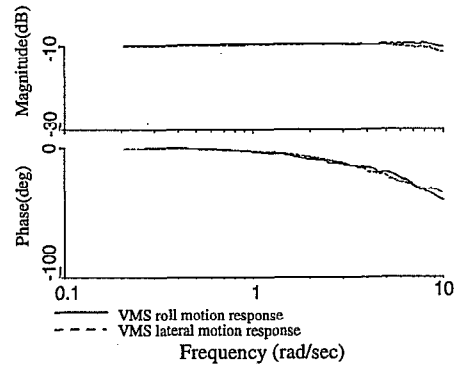


Figure 7. Frequency response of the VMS roll motion response vs. the VMS lateral motion response

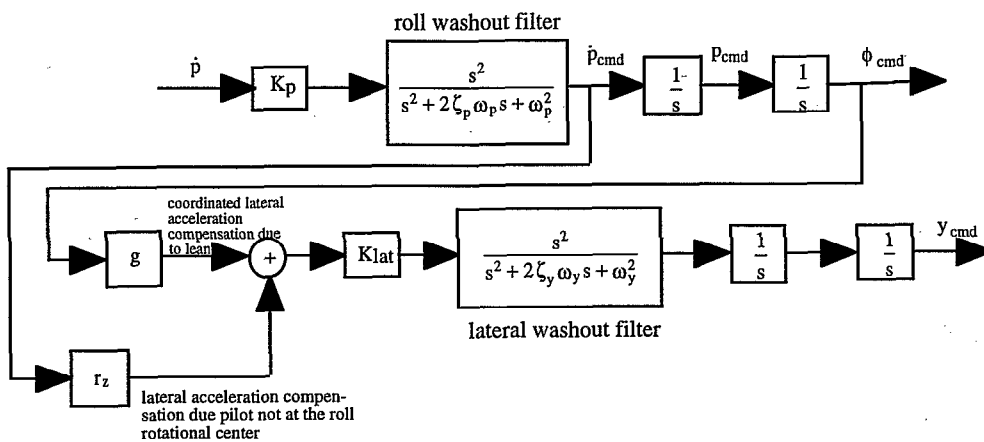
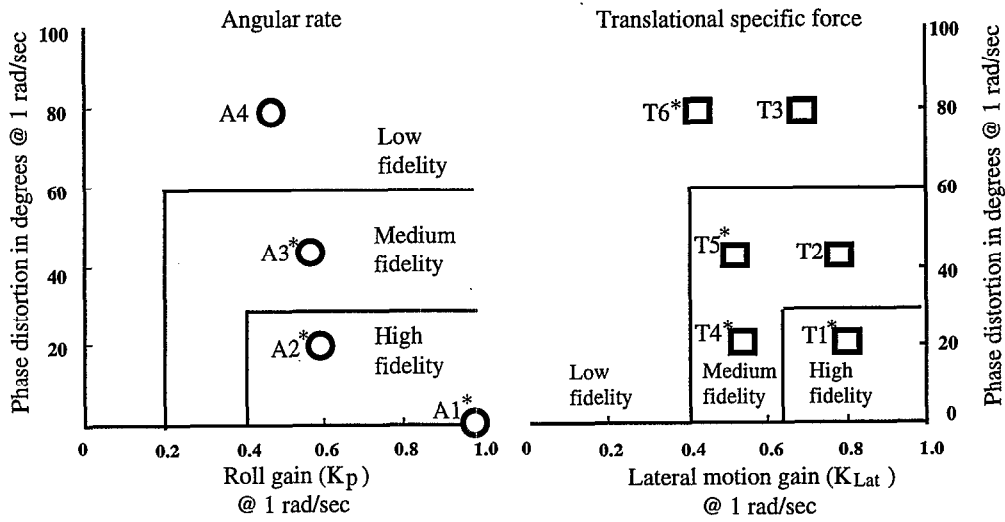
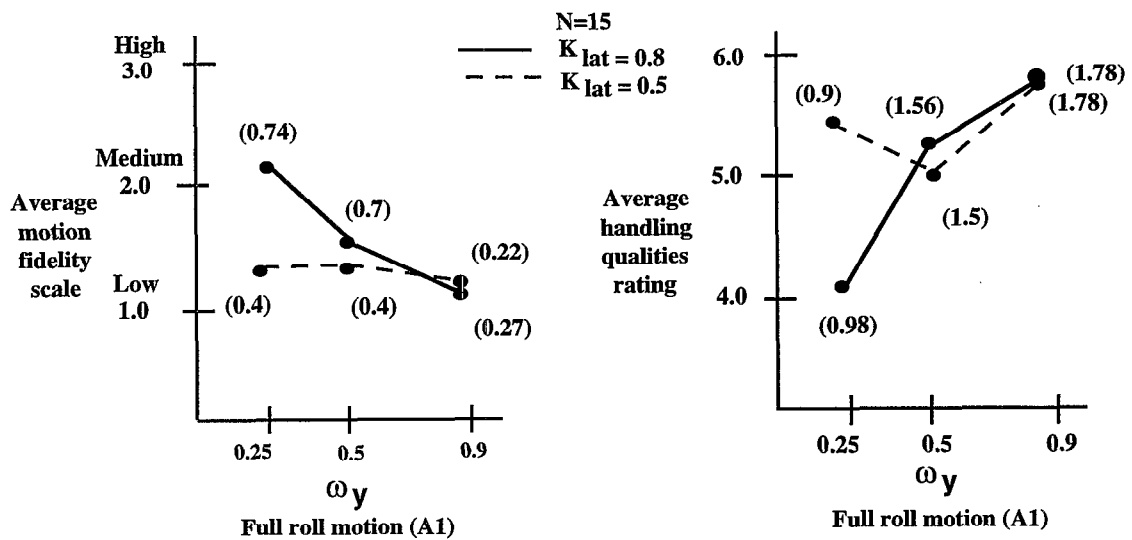


Figure 8. A representative motion drive command block diagram for roll and lateral drives.



* Also tested for the fixed-wing task

Figure 9. Test motion washout filter configurations for the helicopter translational task



N: number of samples
 (*) standard deviation

Figure 10 Combined effects due to lateral gain and phase distortion on the average MFS and HQR for the full motion helicopter task

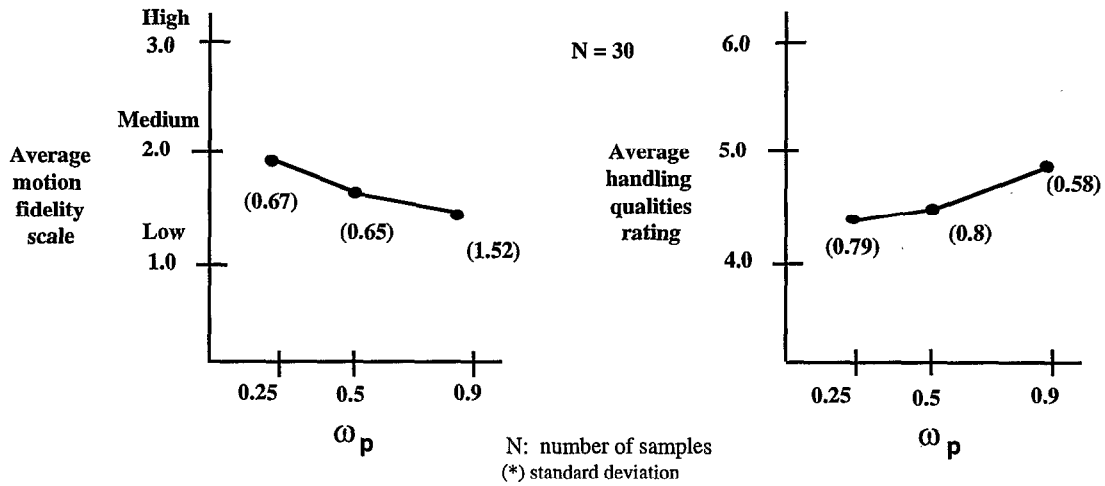


Figure 11. Roll washout filter frequency effect on the average MFS and HQR for the attenuated roll motion in the helicopter task

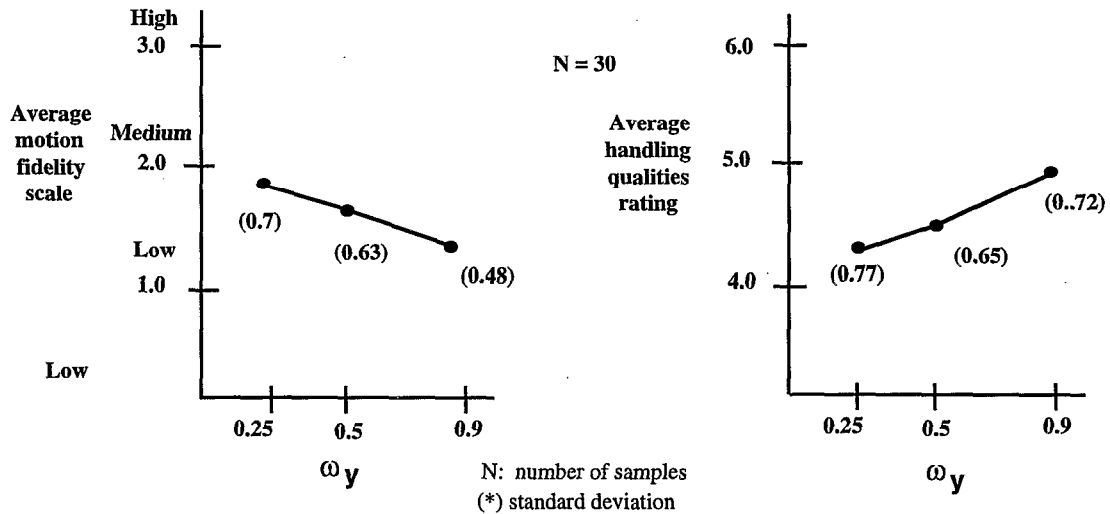


Figure 12. Lateral washout filter frequency effect on the average MFS and HQR for the attenuated roll motion in the helicopter task

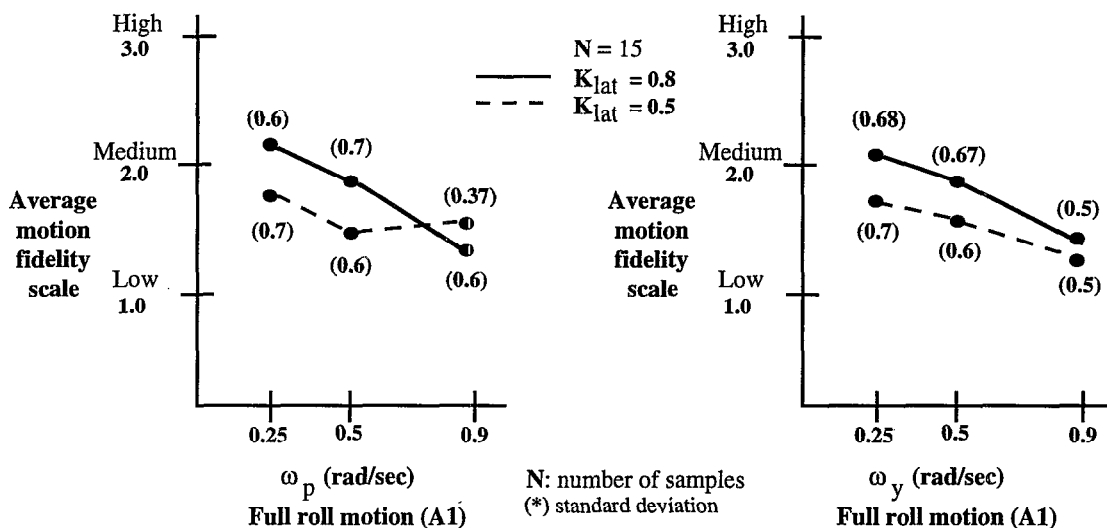


Figure 13. Lateral motion gain effect on the average MFS for the attenuated roll motion in the helicopter task

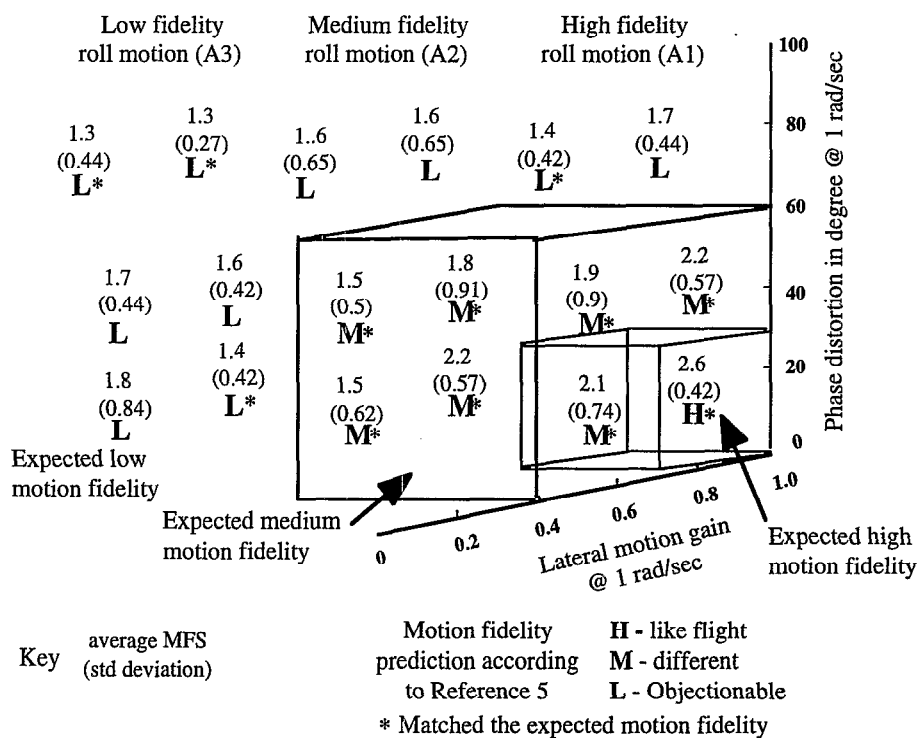


Figure 14. Comparison of the average MFS from the helicopter task with Reference 5

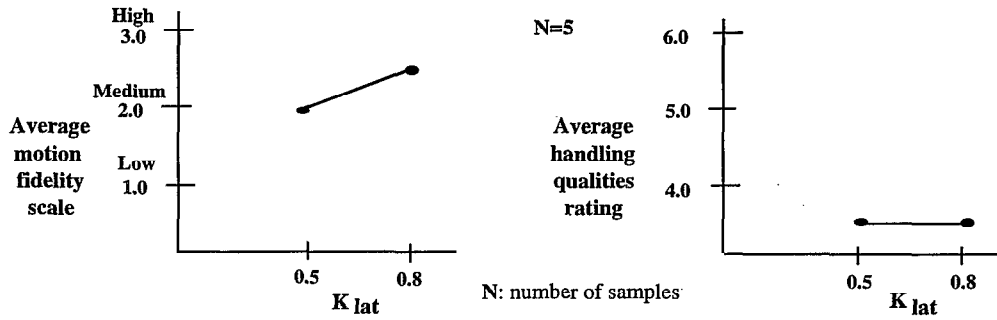


Figure 15. Lateral motion gain effect on the average MFS and HQR for the full roll motion in the fixed wing task

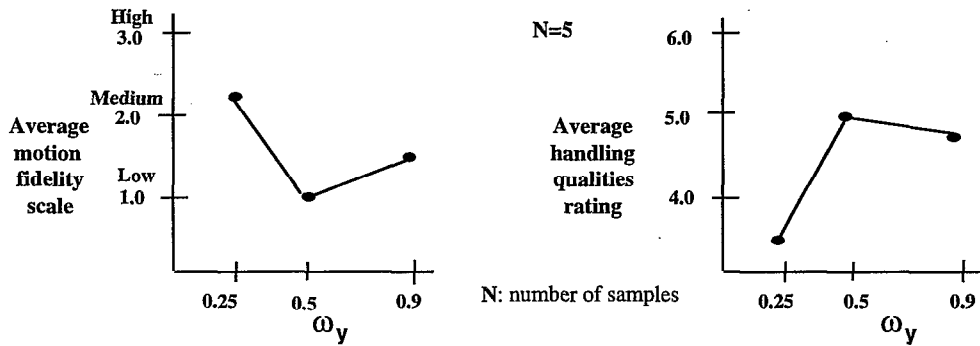


Figure 16. Lateral washout filter frequency effect on the average MFS and HQR for the full roll motion in the fixed wing task

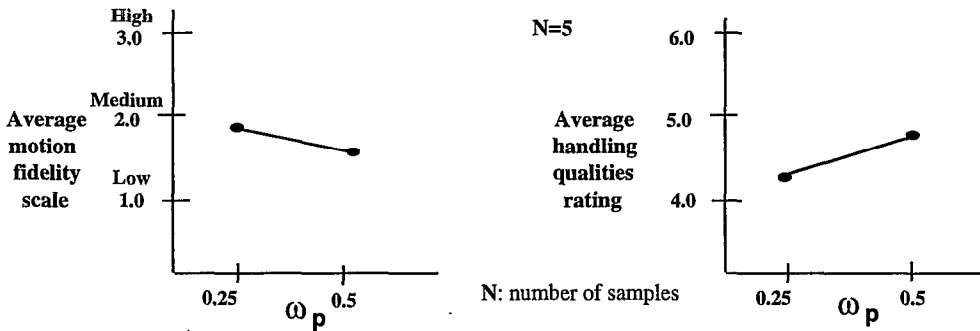


Figure 17. Roll washout filter frequency effect on the average MFS and HQR for the attenuated roll motion in the fixed wing task

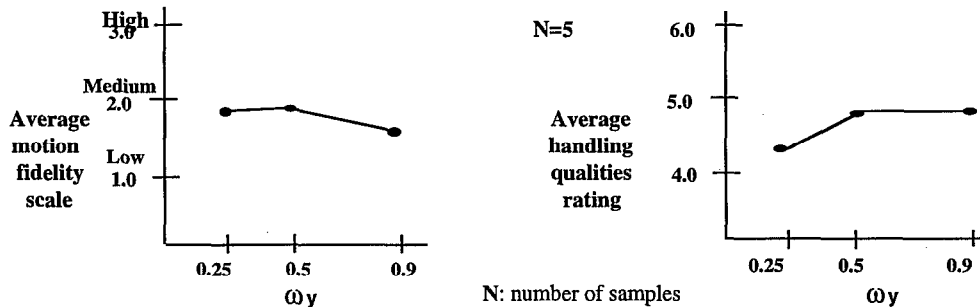


Figure 18. Lateral washout filter frequency effect on the average MFS and HQR for the attenuated roll motion in the fixed wing task